Strong interplay between stripe spin fluctuations, nematicity and superconductivity in FeSe

Qisi Wang, Yao Shen, Bingying Pan, Yiqing Hao, Mingwei Ma, Fang Zhou, P. Steffens, K. Schmalzl, T. Forrest, M. Abdel-Hafiez, et al.

Strong Interplay between Stripe Spin Fluctuations, Nematicity and Superconductivity in FeSe

Qisi Wang,[1] Yao Shen,[1] Bingying Pan,[1] Yiqing Hao,[1] Mingwei Ma,[2] Fang Zhou,[2] P. Steffens,[3] K. Schmalzl,[4] T. R. Forrest,[5] M. Abdel-Hafiez,[6,7] Xiaojia Chen,[6] D. A. Chareev,[8] A. N. Vasiliev,[9,10,11] P. Bourges,[12] Y. Sidis,[12] Huibo Cao,[13] and Jun Zhao*[1,14]

[1] *State Key Laboratory of Surface Physics and Department of Physics, Fudan University, Shanghai 200433, China*

[2] *Beijing National Laboratory for Condensed Matter Physics, Institute of Physics, Chinese Academy of Science, Beijing 100190, China*

[3] *Institut Laue-Langevin, 71 Avenue des Martyrs, 38042 Grenoble Cedex 9, France*

[4] *Juelich Centre for Neutron Science JCNS Forschungszentrum Juelich GmbH, Outstation at ILL, 38042 Grenoble, France*

[5] *European Synchrotron Radiation Facility, BP 220, F-38043 Grenoble Cedex, France*

[6] *Center for High Pressure Science and Technology Advanced Research, Shanghai, 201203, China*

[7] *Faculty of Science, Physics Department, Fayoum University, 63514 Fayoum, Egypt*

[8] *Institute of Experimental Mineralogy, Russian Academy of Sciences, 142432 Chernogolovka, Moscow District, Russia*

[9] *Low Temperature Physics and Superconductivity Department, M.V. Lomonosov Moscow State University, 119991 Moscow, Russia*

[10] *Theoretical Physics and Applied Mathematics Department, Ural Federal University, 620002 Ekaterinburg, Russia*

[11] *National University of Science and Technology "MISiS", Moscow 119049, Russia*

[12] *Laboratoire Leon Brillouin, CEA-CNRS, CEA-Saclay, 91191 Gif sur Yvette, France*

[13] *Neutron Scattering Science Division, Oak Ridge National Laboratory, Oak Ridge, Tennessee 37831-6393, USA*

[14] *Collaborative Innovation Center of Advanced Microstructures, Fudan University, Shanghai 200433, China*

Elucidating the microscopic origin of nematic order in iron-based superconducting materials is important because the interactions that drive nematic order may also mediate the Cooper pairing[1]. Nematic order breaks fourfold rotational symmetry in the iron plane, which is believed to be driven by either orbital or spin degrees of freedom[1–5]. However, as the nematic phase often develops at a temperature just above or coincides with a stripe magnetic phase transition, experimentally determining the dominant driving force of nematic order is difficult[1,6]. Here, we use neutron scattering to

study structurally the simplest iron-based superconductor FeSe (ref. 7), which displays a nematic (orthorhombic) phase transition at $T_s = 90$ K, but does not order antiferromagnetically. Our data reveal substantial stripe spin fluctuations, which are coupled with nematicity and are enhanced abruptly on cooling to below T_s. Moreover, a sharp spin resonance develops in the superconducting state, whose energy (~ 4 meV) is consistent with an electron boson coupling mode revealed by scanning tunneling spectroscopy[8], thereby suggesting a spin fluctuation-mediated sign-changing pairing symmetry. By normalizing the dynamic susceptibility into absolute units, we show that the magnetic spectral weight in FeSe is comparable to that of the iron arsenides[9,10]. Our findings support recent theoretical proposals that both nematicity and superconductivity are driven by spin fluctuations[1,2,11–14].

Most parent compounds of iron-based superconductors exhibit a stripe-type long-range antiferromagnetic (AFM) order which is pre-empted by an electronic nematic order. In analogy to the nematic phase of liquid crystal characterized by molecules that have no positional order but tend to be aligned in the same direction, electronic nematicity is an electronic phase that spontaneously breaks the rotational symmetry while preserving the translation symmetry. Superconductivity emerges when the magnetic and nematic order are partially or completely suppressed by chemical doping or by the application of pressure[1,6]. The stripe AFM order consists of columns of parallel spins along the orthorhombic *b* direction, together with antiparallel spins along the *a* direction. Similar to the stripe AFM order, the nematic order also breaks the fourfold rotational symmetry, which is signaled by the tetragonal to orthorhombic structure phase transition and pronounced in-plane anisotropy of electronic and magnetic properties[1,6,15–18]. It has been proposed that nematicity could be driven either by orbital or spin fluctuations, and that orbital fluctuations tend to lead to a sign-preserving s^{++}-wave pairing, while spin fluctuations favor a sign-changing $s^{\pm}$-wave or *d*-wave pairing[1–6,14,19,20]. However, as orbital and spin degrees of freedom are coupled and could be easily affected by the nearby stripe magnetic order, it remains elusive which of them is the primary driving force of nematicity[1–5,14,19].

FeSe ($T_c \approx 8$ K) has attracted great attention not only because of the simple crystal structure (Fig. 1a), but also because it displays a variety of exotic properties unprecedented for other iron based superconductors. For example, the T_c of FeSe increases to ~40 K under pressure[21] or by ion/molecule intercalation[22]. In addition, the T_c of single layer FeSe thin film is as high as 100 K, which is significantly higher than in other iron based superconductors[23]. More interestingly, unlike most iron-based materials, the tetragonal to orthorhombic structural transition in bulk FeSe is not followed by a stripe magnetic order[7], providing an exciting opportunity to elucidate the microscopic origin of nematicity and its interplay with superconductivity. The absence of stripe magnetic order in FeSe seems to cast doubt on the spin driven nematicity scenario. Moreover, recent nuclear magnetic resonance (NMR) measurements suggested that there were almost no spin fluctuations above T_s in the tetragonal phase, which was also interpreted as a breakdown of the spin scenario[24,25]. However, NMR only probes momentum-integrated spin fluctuations at very low energies ($\sim 0.1\mu$eV or lower). The momentum dependence of the higher energy spin fluctuations-especially at the energy scale close to the superconducting gap, which is believed to be more important in driving nematicity and superconductivity[11,14]-remains unknown. This issue could be addressed by inelastic neutron scattering measurements that probe spin fluctuations over a wide range of momentum and energy.

Neutron scattering studies on FeSe single crystals have been hampered by the lack of high quality samples with the correct phase. Recently, advances in crystal growth with vapor-transport and floating zone techniques have allowed us to grow FeSe single crystals which are significantly larger than what was previously available[26,27]. The superconducting properties of our sample were characterized by DC magnetic susceptibility and resistivity measurements which show an onset T_c of 8.7 K with a transition width of ~0.3 K, indicating the high quality of the sample (Figs. 1b, 1c). Clear kinks on magnetic susceptibility and resistivity associated with the tetragonal to orthorhombic structure transition are also observed close to 90 K. Our single crystal X-ray diffraction refinements suggest that the chemical composition [$FeSe_{0.990(10)}$] is stoichiometric within the error bar and no interstitial atoms or impurity phases are observed. The refined

structure parameters are summarized in STable 1 in the Supplementary Information. We note that the lattice constant of our sample in the c axis is longer than that of the Se deficient sample reported in ref. 28. This is consistent with the trend that the c axis lattice constant increases with increasing Se concentrations[28].

We first use elastic neutron scattering to study the structural and magnetic ordering properties of our FeSe samples. The (4, 0, 0)/(0, 4, 0) peaks below T_s=90 K can be resolved into two distinct peaks, indicative of the structural phase transition from the tetragonal to orthorhombic symmetry (Fig. 2a). On the other hand, no magnetic Bragg peaks associated with the stripe or double stripe magnetic order are observed (not shown) at temperatures down to 1.5 K, consistent with previous measurements of powder samples[7]. Instead, in the inelastic channel, we have observed strong spin fluctuations near (1, 0, 0), which corresponds to the stripe AFM wavevector of the parent compounds of iron-based superconductors[6]. To determine the momentum dependence of the spin fluctuations and their interplay with superconductivity, we performed rocking/transverse and radial/longitudinal **Q**-scans (the scan directions are perpendicular and along **Q**, respectively) below and above T_c. As shown in Figs. 2b, 2d, representative **Q**-scans at 4 meV are commensurate near (1, 0, 0) at T = 11 K in both transverse and longitudinal directions with no observable anisotropy. The peak intensity is drastically enhanced below T_c, which is reminiscent of a magnetic resonant mode observed in other iron-based superconductors[6,9,10,14,29,30]. Conversely, the scattering at 2.5 meV is suppressed upon entering the superconducting state due to the opening of the superconducting spin gap (Fig. 2c). The redistribution of the magnetic spectral weight across T_c indicates that the spin fluctuations near (1, 0, 0) are closely related to superconductivity. In order to clarify the detailed momentum structure of the superconductivity-induced spin fluctuations, we have subtracted the signal of the normal state from that of the superconducting state and plot a 2D contour map interpolated from a series of **Q**-scans at 4 meV (Fig. 2e). The outcome shows that the spin fluctuation spectra are commensurate with little anisotropy (within our instrumental accuracy). In addition to the results shown near (1, 0, 0), we also performed similar measurements in the second magnetic Brillouin zone near (2, 1, 0) associated with the stripe magnetic

structure (Fig. 2e). A similar signal is also observed, but with weaker intensity because of the decreased magnetic form factor. These results unambiguously demonstrate that the scattering that we observe here is pure magnetic fluctuation associated with stripe magnetism rather than phonons as the scattering strength from phonons is related to $(\mathbf{Q}\cdot\xi)^2$, where ξ is the polarization vector of the phonon.

Figure 3 summarized the energy dependence of dynamic spin correlation function $S(\mathbf{Q},\omega)$ at $\mathbf{Q}$=(1, 0, 0) at different temperatures. The figure confirms that the spectral weight loss in the superconducting spin gap (< 3 meV) is compensated by a sharp resonance mode at around 4 meV. Moreover, the detailed temperature dependence of the scattering at 4 meV shows an order-parameter-like behavior and is clearly coupled to the occurrence of superconductivity (Fig. 4a). The spin resonance mode has been interpreted either as a spin exciton within the superconducting gap arising from scattering between portions of the Fermi surface where the superconducting gap function has an opposite sign[14] or as a broad hump structure induced by overshoot in the magnetic spectrum above the superconducting gap in a sign-preserving s^{++} pairing state[20]. The sharp mode that we observed here is consistent with the spin exciton model as the mode energy (4 meV) is below the superconducting gap ($2\Delta\approx5$ meV) (ref. 31), and the energy width (~ 1.2 meV) of the mode is essentially resolution-limited and much sharper than in other iron-based superconductors[6,9,10,14,29,30]. More interestingly, the resonance energy (E_r=4meV$\approx5.3k_BT_c$) is consistent with the electron boson coupling mode (~3.8 meV) revealed by scanning tunneling spectroscopy[8], thereby suggesting strong electron-spin fluctuations coupling in this system. These results are consistent with a spin fluctuation-mediated sign changing pairing mechanism, but inconsistent with an orbital fluctuations-mediated sign-preserving s^{++}-wave pairing mechanism[14,20,32].

Although commensurate stripe spin fluctuations persist at all temperatures measured, the system remains paramagnetic at low temperature. Theoretically, it has been shown that the magnetic interactions in FeSe are more frustrated than in iron arsenides and therefore prevent long-range magnetic order[11–13]. Hence, it is informative to compare the magnetic spectral weight in FeSe with that of iron arsenide superconductors.

We have calculated absolute units of the imaginary part of the dynamic susceptibility $\chi''(\mathbf{Q},\omega)$ by normalizing $S(\mathbf{Q},\omega)$ for the thermal population factor and the intensity of acoustic phonons (Fig. 3b and the Supplementary Information). The outcome reveals that the integrated resonance spectral weight (0.00212 μ_B^2/Fe) is about 30% of that in the carrier doped $BaFe_{1.85}Co_{0.15}As_2$ (E_r = 9.5 meV) (ref. 9), but two times larger than the damped resonance mode in the isovalently doped $BaFe_{1.85}Ru_{0.15}As_2$ (T_c=14 K, E_r = 5.5 meV) (ref. 10). Since the T_c (8.7 K) of FeSe is also about a factor of three lower than in $BaFe_{1.85}Co_{0.15}As_2$ (T_c = 25 K), the overall magnetic spectral weight in both systems are comparable.

Having established the interplay between the spin fluctuations and superconductivity, we now turn to the impact of nematicity on the spin fluctuations. Previous NMR measurements suggested the absence of spin fluctuations above T_s in the tetragonal phase[24,25]. In contrast, our neutron scattering measurements show substantial spin fluctuations in the tetragonal phase (T = 110 K) (Figs. 3a, 2d). We note that the energy dependence of the dynamical spin correlation function $S(\mathbf{Q},\omega)$ displays a spin gap-like feature at low energies at T = 110 K (Fig. 3a), which is confirmed by the featureless $\mathbf{Q}$-scan at 2.5 meV (Fig. 2c). These results agree with a theoretically predicted gapped nematic quantum paramagnetic state, where frustrated magnetic correlation is the driving force of nematicity and is responsible for the lack of long-range magnetic order in FeSe (ref. 11). This naturally accounts for the absence of low energy spin fluctuations above T_s suggested by NMR measurements[24,25]. The most striking observation is that the spin fluctuations are enhanced abruptly in the orthorhombic phase at T = 11 K (Fig. 3a). We note that the spin fluctuation enhancement is more pronounced at lower energies, suggesting a slowing down of spin fluctuations. This indicates that the system is closer to the stripe magnetic ordered state at low temperature. To determine if the increase of the spin fluctuation is indeed associated with the nematic order, we carefully measured the temperature dependence of the scattering at 2.5 meV, which is the lowest energy that can be measured in our thermal triple axis spectrometer with a reasonable background. Intriguingly, a comparison of the temperature evolution of the $S(\mathbf{Q},\omega)$ with the orthorhombicity $\delta(T) = (a - b)/(a + b)$ reveals that the

enhancement of the $S(\mathbf{Q},\omega)$ is clearly coupled to the development of the nematic (orthorhombic) phase (Fig. 4b). These results are consistent with the recent proposals (based on either itinerant or local moment pictures) that the nematic order is driven by spin fluctuations[1,2,11–13]. In a local moment model that frustrated magnetic interactions drive nematic order in FeSe, once the orthorhombic distortion develops, it lifts the magnetic frustration, therefore making the system move toward the stripe ordered phase. As a result the spin fluctuations at the stripe ordering wavevector are enhanced. On the other hand, a sharp enhancement of spin fluctuations at T_s is not predicted in a simple orbital-driven nematicity model[25].

It is interesting to compare the spin fluctuations of FeSe with that of the iron selenide superconductors with higher T_c, but without nematic order. The low energy spin fluctuations in $FeTe_{1-x}Se_x$ (T_c=14 K) and $Rb_xFe_{2-y}Se_2$ (T_c=32 K) appear at $\mathbf{Q}$=$(1, -0.3 \leq \xi \leq 0.3)$ and $\mathbf{Q}$=$(1, \pm 0.5)$, respectively[29,30,33]. Different from FeSe, the dynamic spin correlation $S(\mathbf{Q},\omega)$ of $FeTe_{1-x}Se_x$ displays little temperature dependence from T_c to 300 K (ref. 29). Moreover, the spin fluctuations of $FeTe_{1-x}Se_x$ are broad and incommensurate/anisotropic[29,30], in contrast to the relatively sharp and commensurate spin fluctuations at the stripe AFM wavevector in FeSe. Therefore, FeSe is closer to the stripe magnetic instability and consequently with a larger spin-spin correlation length. These results further imply that nematicity is driven by stripe spin fluctuations, though superconductivity can be mediated by spin fluctuations either at or away from the stripe AFM wavevector.

In summary, we have reported evidence of strong coupling between the stripe spin fluctuations, nematicity and superconductivity in single crystalline FeSe. Contrary to earlier NMR measurements[24,25], our neutron scattering data reveal substantial commensurate stripe spin fluctuations in the tetragonal phase, which are coupled with orthorhombicity and abruptly enhanced in the nematic phase. This is not predicted in a simple orbital-driven nematicity model[25]. Moreover, a resolution-limited sharp spin resonance appears well below the superconducting gap and is coupled with electronic density of states, indicating a spin fluctuations-mediated sign-changing pairing symmetry rather than an orbital fluctuations-mediated

sign-preserving s^{++}-wave pairing symmetry. These results are in agreement with the theoretical predictions that nematicity and superconductivity are driven by spin fluctuations[1,2,11–14], and will be critical in identifying the microscopic paring mechanism of this system. The elucidation of the interplay between spin fluctuations, nematicity and superconductivity will also have important implications for the understanding of other exotic properties of iron selenide superconductors, such as the drastically increased T_c under substrate strain/external pressure or by ion/molecule intercalation[21–23].

Note added: After we finished this paper, we became aware of a related preprint describing neutron scattering measurements on FeSe powder samples[34].

*Correspondence and requests for materials should be addressed to J.Z. (zhaoj@fudan.edu.cn).

Acknowledgements

We thank D. H. Lee, Q. Si, F. Wang and H. Yao for useful discussions. This work is supported by the National Natural Science Foundation of China (Grant No. 11374059) and the Shanghai Pujiang Scholar Program (Grant No.13PJ1401100). M.M. and F.Z. acknowledge support from National Natural Science Foundation of China (Grant No. 11190020). H.C. received support from the Scientific User Facilities Division, Office of Basic Energy Sciences, U.S. Department of Energy. A.N.V. was supported in part from the Ministry of Education and Science of the Russian Federation in the framework of Increase Competitiveness Program of NUST ⟨MISiS⟩ (No. 2-2014-036). D.A.C. and A.N.V. acknowledge also support of Russian Foundation for Basic Research through Grants 13-02-00174, 14-02-92002, 14-02-92693.

Author contributions

J.Z. planned the project. M.M., F.Z., D.A.C. and A.N.V. synthesized the sample. Q.W., Y.Shen, B.P., Y.H., M.A. and X.C. characterized the sample. Q.W. and Y.Shen. carried out the neutron experiments with experimental assistance from P.S., K.S., T.R.F., P.B., Y.Sidis and H.C. J.Z. and Q.W. analysed the data and wrote the paper. All authors provided comments for the paper.

Additional information

The authors declare no competing financial interests. Supplementary information accompanies this paper on www.nature.com/naturematerials. Reprints and permission information is available online at http://www.nature.com/reprints. Correspondence and requests for materials should be addressed to J.Z.

References

[1] see Fernandes, R. M., Chubukov, A. V. & Schmalian, J. What drives nematic order in iron-based superconductors? *Nature Phys.* **10**, 97-104 (2014), and references there-in.

[2] Fernandes, R. M. et al. Preemptive nematic order, pseudogap, and orbital order in the iron pnictides. *Phys. Rev. B* **85**, 024534 (2012).

[3] Fang, C., Yao, H., Tsai,W-F., Hu, J. & Kivelson, S. A. Theory of electron nematic order in LaFeAsO. *Phys. Rev. B* **77**, 224509 (2008).

[4] Xu, C., Muller, M. & Sachdev, S. Ising and spin orders in the iron-based superconductors. *Phys. Rev. B* **78**, 020501(R) (2008)

[5] Kruger, F., Kumar, S., Zaanen, J. & van den Brink, J. Spin-orbital frustrations and anomalousmetallic state in iron-pnictide superconductors. *Phys. Rev. B* **79**, 054504 (2009).

[6] see Dai, P. C., Hu, J. P. & Dagotto, E. Magnetism and its microscopic origin in iron-based high-temperature superconductors. *Nature Phys.* **8**, 709-718 (2012), and references there-in.

[7] McQueen, T. M. et al. Tetragonal-to-orthorhombic structural phase transition at 90 K in the superconductor $Fe_{1.01}Se$. *Phys. Rev. Lett.* **103**, 057002 (2009).

[8] Song, C. L. et al. Imaging the electron-boson coupling in superconducting FeSe films using a scanning tunneling microscope. *Phys. Rev. Lett.* **112**, 057002 (2014).

[9] Inosov D. S. et al. Normal-state spin dynamics and temperature-dependent spin-resonance energy in optimally doped $BaFe_{1.85}Co_{0.15}As_2$. *Nature Phys.* **6** 178-181 (2010)

[10] Zhao, J., et al. Effect of electron correlations on magnetic excitations in the isovalently doped iron-based superconductor $Ba(Fe_{1-x}Ru_x)_2As_2$. *Phys. Rev. Lett.* **110**, 147003 (2013)

[11] Wang, F., Kivelson S. & Lee, D. H. Is FeSe a nematic quantum paramagnet? Preprint at ⟨ http://arxiv.org/abs/1501.00844⟩ (2015).

[12] Glasbrenner, J. K., et al. Effect of magnetic frustration on nematicity and superconductivity in Fe chalcogenides. Preprint at ⟨ http://arxiv.org/abs/1501.04946⟩ (2015).

[13] Yu, R. & Si, Q. M. Antiferroquadrupolar and Ising-nematic orders of a frustrated bilinear-biquadratic Heisenberg model and implications for the magnetism of FeSe. Preprint at ⟨ http://arxiv.org/abs/1501.05926⟩ (2015).

[14] see Scalapino, D. J. A common thread: The pairing interaction for unconventional superconductors. *Rev. Mod. Phys*. **84**, 1383 (2012), and references there-in.

[15] Chuang, T-M. et al. Nematic electronic structure in the parent state of the iron-based superconductor $Ca(Fe_{1-x}Co_x)_2$ As_2. *Science* **327**,

181-184 (2010).

[16] Lu, X. Y. et al. Nematic spin correlations in the tetragonal state of uniaxial-strained $BaFe_{2-x}Ni_xAs_2$. *Science* **345**, 657-660 (2014).

[17] Yi, M. et al. Symmetry-breaking orbital anisotropy observed for detwinned $Ba(Fe_{1-x}Co_x)_2As_2$ above the spin density wave transition. *Proc. Natl Acad. Sci. USA* **108**, 6878-6883 (2011).

[18] Chu, J-H., Kuo, H-H., Analytis, J. G. & Fisher, I. R. Divergent nematic susceptibility in an iron arsenide superconductor. *Science* **337**, 710-712 (2012).

[19] Zhang, Q. et al. Neutron-scattering measurements of the spin excitations in LaFeAsO and $Ba(Fe_{0.953}Co_{0.047})_2As_2$: Evidence for a sharp enhancement of spin fluctuations by nematic order. Preprint at ⟨ http://arxiv.org/abs/1410.6855⟩ (2015).

[20] Kontani, H. & Onari, S. Orbital-fluctuation-mediated superconductivity in iron pnictides: analysis of the five-orbital Hubbard-Holstein model. *Phys. Rev. Lett.* **104**, 157001 (2010).

[21] Medvedev, S. et al. Electronic and magnetic phase diagram of β-$Fe_{1.01}Se$ with superconductivity at 36.7 K under pressure. *Nature Mater.* **8**, 630-633 (2009).

[22] Guo, J. G. et al. Superconductivity in the iron selenide $K_xFe_2Se_2$($0 \leq x \leq 1.0$). *Phys. Rev. B* **82**, 180520(R) (2010).

[23] Ge, J-F. et al. Superconductivity above 100 K in single-layer FeSe films on doped $SrTiO_3$. *Nature Mater.* **14**, 285-289 (2015).

[24] Bohmer. A. E. et al. Origin of the tetragonal-to-orthorhombic phase transition in FeSe: A combined thermodynamic and NMR study of nematicity. *Phys. Rev. Lett.* **114**, 027001 (2015).

[25] Baek, S-H. et al. Orbital-driven nematicity in FeSe. *Nature Mater.* **14**, 210-214 (2015).

[26] Chareev, D. et al. Single crystal growth and characterization of tetragonal $FeSe_{1-x}$ superconductors. *Cryst. Eng. Comm.* **15**, 1989 (2013).

[27] Ma, M. W. et al. Flux-free growth of large superconducting crystal of FeSe by traveling-solvent floatingzone technique. *Supercond. Sci. Technol.* **27**, 122001 (2014).

[28] Hsu, F. C. et al. Superconductivity in the PbO-type structure α-FeSe. *Proceedings of the National Academy of Sciences* **105**,14262-14264 (2008).

[29] Xu, Z. J. et al. Local-moment magnetism in superconducting $FeTe_{0.35}Se_{0.65}$ as seen via inelastic neutron scattering. *Phys. Rev. B* **84**, 052506 (2011).

[30] Qiu, Y. M. et al. Spin gap and resonance at the nesting wave vector in superconducting $FeSe_{0.4}Te_{0.6}$. *Phys. Rev. Lett.* **103**, 067008 (2009).

[31] Kasahara, S. et al. Field-induced superconducting phase of FeSe in the BCS-BEC cross-over. *Proc. Natl Acad. Sci. USA* **111**, 16309-16313 (2014).

[32] Zhang, C. L. et al. Distinguishing $s^{\pm}$ and s^{++} electron pairing symmetries by neutron spin resonance in superconducting $NaFe_{0.935}Co_{0.045}As$. *Phys. Rev. B* **88** 064504 (2013).

[33] Park, J. T. et al. Magnetic resonant mode in the low-energy spin-excitation spectrum of superconducting $Rb_2Fe_4Se_5$ single crystals. *Phys. Rev. Lett.* **107**, 177005 (2011).

[34] Rahn, M. C. et al. Strong (π,0) spin fluctuations in β-FeSe observed by neutron spectroscopy. Preprint at ⟨ http://arxiv.org/abs/1502.03838⟩

(2015).

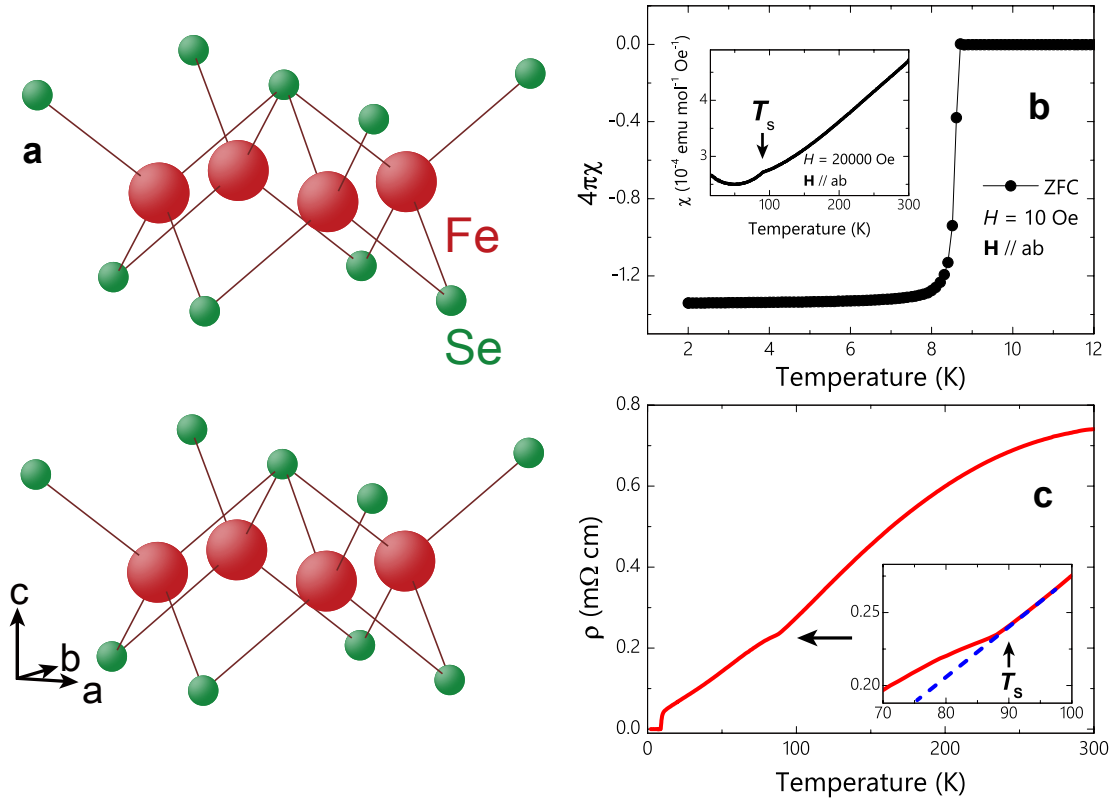

Figure 1: **Orthorhombic crystal structure, magnetic susceptibility and resistivity of FeSe single crystal**. **a**, Schematic diagram of FeSe crystal structure. **b**, The DC magnetic susceptibility measurements on the single-crystalline FeSe sample. A sharp superconducting transition is observed at T_c = 8.7 K in the ZFC measurement in a magnetic field of H = 10 Oe, indicating ~ 100% exclusion of the external magnetic field. The screening is slightly larger than −1 because of the demagnetization effect. The inset shows the susceptibility measured in a magnetic field of H = 20 kOe. The magnetic fields are applied perpendicular to the c axis. **c**, In-plane resistivity as a function of temperature. The inset shows data around T_s = 90 K on an enlarged scale.

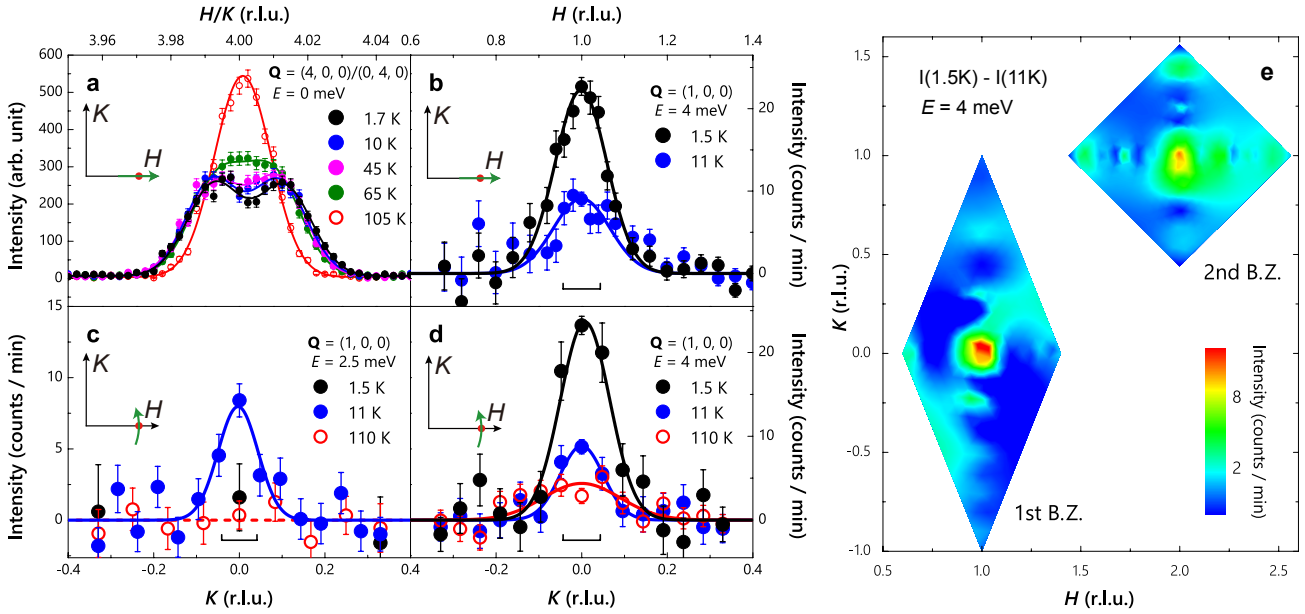

Figure 2: **Structure phase transition and momentum dependence of the spin fluctuations at various temperatures in FeSe**. The inelastic neutron scattering measurements were carried out for the neutron energy loss convention (energy is transferred from the neutron to sample) on the IN20 thermal triple axis spectrometer at the Institut Laue-Langevin, Grenoble, France and the 2T1 thermal triple axis spectrometer at the Laboratoire Leon Brillouin, France. The FeSe single crystals are co-aligned in the (H, K, 0) horizontal scattering plane within ~ 3 degrees mosaicity for the measurements. The elastic measurements were performed on one piece of small single crystal on the 4F2 cold triple axis spectrometer at the Laboratoire Leon Brillouin, France (the instrument configurations are described in the Supplementary Information). We present the data by defining the wave vector **Q** at (q_x, q_y, q_z) as (h, k, l)= ($q_x a/2\pi$, $q_y a/2\pi$, $q_z c/2\pi$) reciprocal lattice units (r.l.u.) in the orthorhombic unit cell. **a**, Temperature dependence of the (4, 0, 0)/(0, 4, 0) nuclear reflections. **b-d**, **Q**-scans near (1, 0, 0) at various energies and temperatures; linear backgrounds are subtracted (see the Supplementary Information). The scan directions are marked by green arrows in the insets. The fitted peak center at 4 meV and 1.5 K is **Q**=(0.998 ± 0.003, 0.008 ± 0.007, 0), i.e., commensurate within error bar. The horizontal bars indicate the instrument resolution. **e**, 2D contour plot of the temperature difference scattering $[S(1.5K) - S(11K)]$ interpolated from a series of **Q**-scans at 4 meV. The error bars indicate one standard deviation.

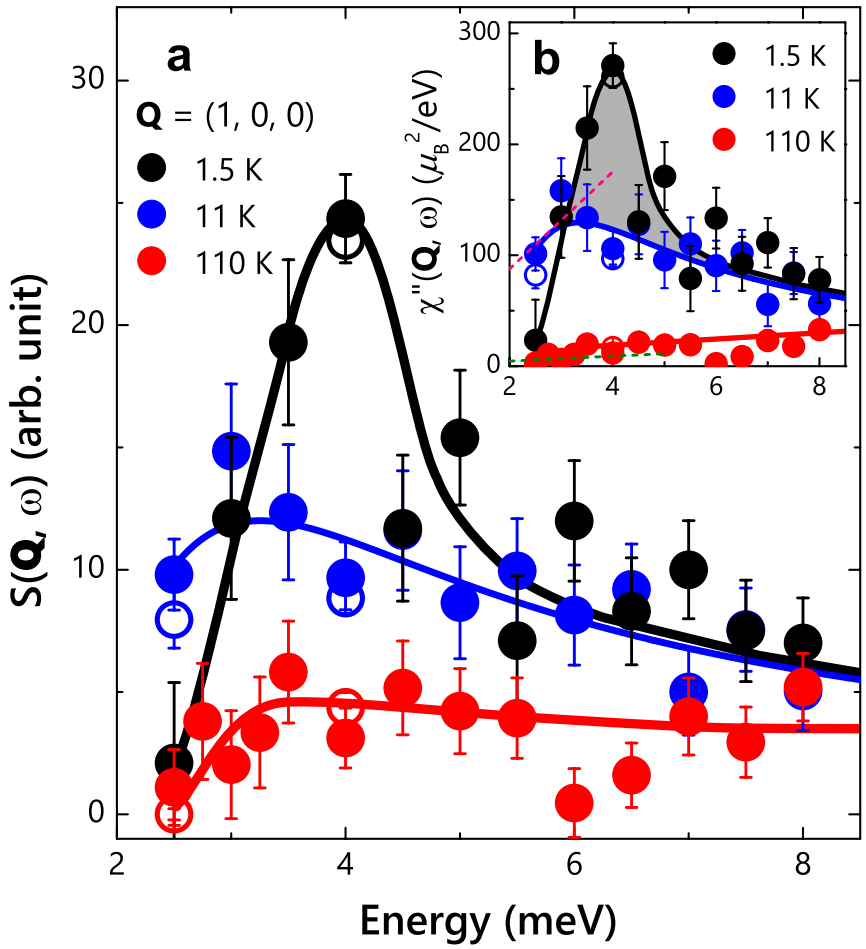

Figure 3: **Energy dependence of spin fluctuations for FeSe in the superconducting state** (T = 1.5 **K) and normal state** (T = 11 **and** 110 **K) a**, Energy dependence of the dynamic spin correlation function $S(\mathbf{Q},\omega)$ at **Q** =(1, 0, 0) after a background correction. The background is measured at **Q** = (0.944, 0.330, 0) and **Q** = (0.944, −0.330, 0), which are on both sides of the magnetic peak in the rocking scan (see Figs. 2c, 2d and the Supplementary Information). The open circles are data fitted with **Q**-scans. **b**, Energy dependence of the imaginary part of the dynamic susceptibility $\chi''(\mathbf{Q},\omega)$ in the superconducting state (T = 1.5 K), and the normal state (T = 11 K). The data are obtained from $S(\mathbf{Q},\omega)$ by correcting for the Bose-population factor and are normalized to absolute units with acoustic phonons as described in the Supplementary Information. The solid curves are guides to the eye. The shaded area denotes the resonance spectral weight. The dashed lines indicate the slope of $\chi''(E)/E$ for $E \rightarrow 0$, which is related to the spin-lattice relaxation rate measured by NMR. The error bars indicate one standard deviation.

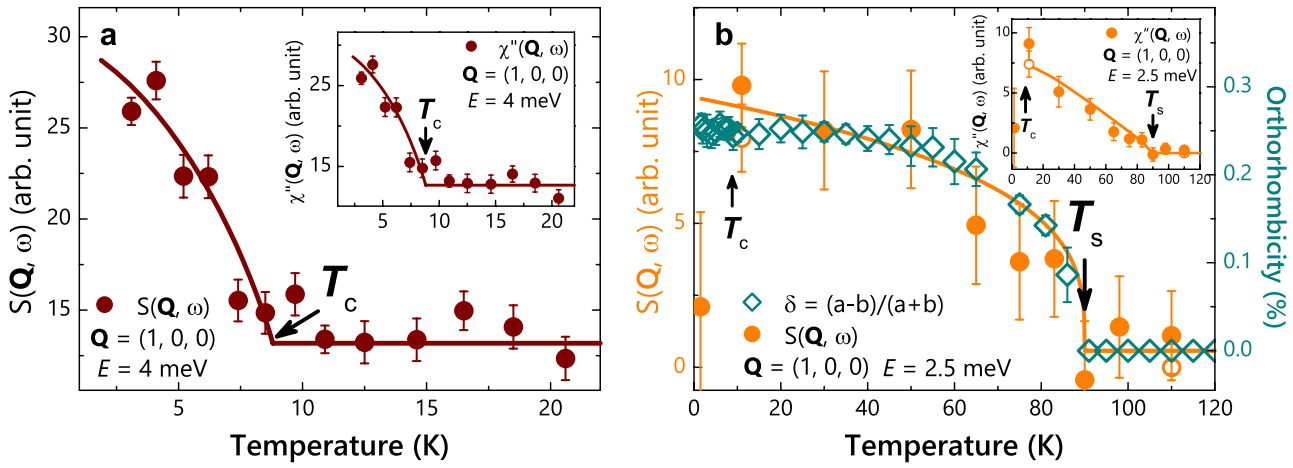

Figure 4: **Temperature dependence of spin fluctuations in FeSe.** **a**, Temperature dependence of dynamic spin correlation $S(\mathbf{Q},\omega)$ at $E = 4$ meV, which clearly shows a kink at T_c. The inset displays the temperature evolution of $\chi''(\mathbf{Q},\omega)$. **b**, Temperature dependence of $S(\mathbf{Q},\omega)$ at $E = 2.5$ meV and the orthorhombicity $\delta(T) = (a - b)/(a + b)$ shows an order-parameter-like behavior with an onset at T_s. The orthorhombicity is determined by the high resolution neutron diffraction data in Fig. 2a and SFig. 5 of the Supplementary Information. The temperature dependence of the orthorhombicity near T_s can be fitted by a simple power law $\delta(T)=\delta_0(1 - T/T_s)^{2\beta}$, where $\beta = 0.15 \pm 0.017$. Although NMR measurements have demonstrated the competition between nematicity and superconductivity in FeSe (ref. 25), the suppression of orthorhombicity below T_c is not clearly observable for our neutron data, probably due to the intrinsic weak effect and resolution constraint. We note that the decrease of the scattering intensity at 2.5 meV and 1.5 K is due to the opening of the superconducting spin gap (Fig. 3). The suppressed spectral weight at 2.5 meV is compensated by the resonance mode at 4 meV, so the total spectral weight only displays a weak change across T_c. Therefore, this does not conflict with the very weak suppression of the orthorhombicity below T_c in the spin driven nematicity scenario. The inset shows the temperature evolution of $\chi''(\mathbf{Q},\omega)$ which also displays a kink at T_s. The open circles are data fitted with **Q**-scans. The solid lines are a guide to the eye. The error bars indicate one standard deviation.